

Accepted Manuscript

Mechanical properties of reinforced composite materials under uniaxial and planar tension loading regimes measured using a non-contact optical method

Mohamed Milad, Sarah Green, Jianqiao Ye

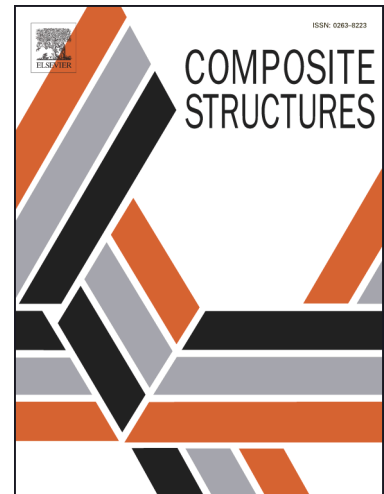
PII: S0263-8223(18)30252-6
DOI: <https://doi.org/10.1016/j.compstruct.2018.05.070>
Reference: COST 9709

To appear in: *Composite Structures*

Received Date: 15 January 2018

Revised Date: 11 May 2018

Accepted Date: 17 May 2018



Please cite this article as: Milad, M., Green, S., Ye, J., Mechanical properties of reinforced composite materials under uniaxial and planar tension loading regimes measured using a non-contact optical method, *Composite Structures* (2018), doi: <https://doi.org/10.1016/j.compstruct.2018.05.070>

This is a PDF file of an unedited manuscript that has been accepted for publication. As a service to our customers we are providing this early version of the manuscript. The manuscript will undergo copyediting, typesetting, and review of the resulting proof before it is published in its final form. Please note that during the production process errors may be discovered which could affect the content, and all legal disclaimers that apply to the journal pertain.

Mechanical properties of reinforced composite materials under uniaxial and planar tension loading regimes measured using a non-contact optical method

Mohamed Milad^{1,2}, Sarah Green¹ and Jianqiao Ye¹

¹Lancaster University, Engineering Department, Gillow Avenue, Lancaster LA1 4YW

²Physics Department, Toubrk University, Toubrk, Libya

Abstract

This study reports the hyperelastic material behaviour of a commercially available PVC/nitrile elastomer with woven continuous nylon reinforcement composite sheet under loading cases of uniaxial extension and pure shear achieved via wide strip tension testing. Through the novel use of an advanced non-contact optical strain measurement technique, the hyperelastic material behaviour of the composite is investigated, and materials parameters are reported for both the warp and the weft directions of reinforcement fibre alignment. The non-contact technique is used to acquire normal and shear strains at the surface of the composite sheet material when loaded to tensile strains (stretches) of up to 0.25. Directly measured shear strains are compared to those derived from the normal strain outputs of an optical rectangular strain rosette array, with both measures showing close agreement. The measured mechanical behaviour under loading is used to determine an approximate strain energy function for the composite via ABAQUS software hyperelastic materials modelling curve fitting, with the Ogden and Yeoh hyperelastic models showing reasonable agreement to experimental data.

1. Introduction

Fabric-reinforced rubber elastomeric composites play an important part in many engineering applications including those in the petroleum, marine, aerospace, transport and gas distribution industries. One appealing property of rubbers is the capacity to bear large temporary deformations with no significant permanent deformation upon load removal (Treloar, 1973). This stress-strain behaviour is usually highly non-linear and is described as hyperelastic, and is characterised by the absence of a single, well-defined modulus of elasticity. Therefore, the characterization of hyperelastic behaviour exhibited by non-linearly elastic materials has practical significance (Shahzad, et al., 2015). Much work has been carried out in the subject area of rubber elasticity, (Jones and Treloar, 1975) with statistically based models and phenomenological approaches reported in the literature. From these early works, using strain energy density functions, a number of constitutive hyperelastic materials

models have been developed to describe large non-elastic deformations of these materials (Gent, 1992).

Industrial uses of rubber elastomer carcass, woven fabric reinforced composites are extensive and because of the wide variety of their applications, there are interests in the use of experimental techniques to determine in-service mechanical performance (Yang et al., 2016). Reinforcement fabrics, which can be woven or nonwoven, include natural filaments or man-made materials such as glass fibres, polyesters or nylons. Typical carcass materials include neoprenes, silicones and butyl rubbers (Testa and Yu, 1987; Reese et al., 2001). For woven textile reinforcements, the textile yarn orientation is a function of the method of manufacture and the textile architecture. If warp yarns are defined as oriented in the axial/lengthwise direction of the textile, then the weft yarns are woven across the warp yarns, running in the transverse direction. The load deflection response of a woven textile is a function of the yarn material properties and also the overall textile architecture (Jacobsen et al, 2004). Industrially, to afford protection to the yarns from both mechanical abrasion and chemical degradation, textiles are commonly coated or moulded within an elastomeric carcass. Synthetic rubbers such as PVC/nitrile composites have enhanced thermal stability and excellent ozone and oil resistance, making these types of fibre filled composites commonplace in the petrochemical industries (Hardiman, 2000). However, experimentally it can prove difficult to adequately capture the non-linear mechanical behaviour of such fabric reinforced elastomers, such as would be required for the data-set inputs for constitutive materials modelling.

By conducting uniaxial and pure shear testing, and the recording of the resultant sample deformation using a non-contacting digital image correlation based video extensometer, this paper reports an investigation into the mechanical properties of a PVC/nitrile with filament nylon composite tyre fabric. The tests demonstrate the suitability of the non-contact optical technique for the capture of hyperelastic material behaviour during loading and enable comparisons between several hyperelastic materials models using ABAQUS curve-fitting methods, with the objective of simplifying the choice of a hyperelastic model and the determination of its constants for a particular material.

2. Hyperelastic material models

Constitutive materials models describing hyperelasticity can be formulated in terms of a strain energy function that depends upon the principal stretches, or invariants, of the strain tensor. The strain energy function (W), is directly linked to the material's stress-strain

response, and depends upon a series of parameters (or material constants). In order to describe a given material behaviour using a particular hyperelastic material model, the material constants must be determined by means of curve fitting to experimentally obtained stress-strain data.

W describes the amount of energy stored in the deformed hyperelastic material as a function of strain at that point in the material (Boyce and Arruda 2000; Shahzad, et al., 2015; Ali et al, 2010; ABAQUS Theory Manual, 1992) and can be written as

$$W = W(I_1, I_2, I_3)$$

(1)

Where I_1, I_2 and I_3 are the three strain invariants of the Green deformation tensor. The strain invariants can be described in terms of the principal stretches, λ_1, λ_2 and λ_3 according to

$$\begin{aligned} I_1 &= \lambda_1^2 + \lambda_2^2 + \lambda_3^2 \\ I_2 &= \lambda_1^2 \lambda_2^2 + \lambda_2^2 \lambda_3^2 + \lambda_3^2 \lambda_1^2 \\ I_3 &= \lambda_1^2 \lambda_2^2 \lambda_3^2 \end{aligned} \quad (2)$$

This enables the strain energy function (1) to be written as

$$W = \sum_{i+j+k=1}^{\infty} C_{ijk} (I_1 - 3)^i \cdot (I_2 - 3)^j \cdot (I_3 - 1)^k \quad (3)$$

Where C_{ijk} are the material-specific constants. If incompressibility is assumed, $I_3=1$ and equation (3) can be further simplified to

$$W = \sum_{i+j=1}^{\infty} C_{ij} (I_1 - 3)^i \cdot (I_2 - 3)^j \quad (4)$$

Many specific hyperelastic materials models have been proposed (Boyce and Arruda, 2000; Seibert and Schoche, 2000) and software such as ABAQUS contains curve fitting routines for several hyperelastic strain energy functions, including those attributed to Mooney-Rivlin, Neo-Hookean, Polynomial, Ogden and Yeoh. Because these functions assume an isotropic hyperelastic material response, they are limited when applied to the modelling of anisotropic hyperelasticity, such as that demonstrated by a hyperelastic matrix (ground substance) when reinforced with a non-hyperelastic fibre phase. In such materials, as the fibre phase fraction increases, the isotropic hyperelastic contribution from the matrix to overall material behaviour diminishes, necessitating a more complex anisotropic hyperelastic material model in order to adequately to describe the material (Holzapfel et al, 2000; Aboshio et al., 2014).

2.1 Ogden model

The Ogden model (Ogden, 1972) is a phenomenological model based on principal stretches rather than invariants. It is able to accurately capture upturn (stiffening) of the stress-strain curve and model rubber over large ranges of deformation. There is good observational agreement between the Ogden model and Treloar's experimental data for unfilled rubber for extensions of up to 700% (Ogden, 1972; Treloar, 1958). The model is defined

$$W = \sum_{i=1}^N \frac{2\mu_i}{\alpha_i^2} (\lambda_1^{\alpha_i} + \lambda_2^{\alpha_i} + \lambda_3^{\alpha_i} - 3) \quad (5)$$

Where μ_i , α_i are temperature-dependent material properties.

2.2 Yeoh model

Yeoh proposed a phenomenological model in the form of a third-order polynomial based only on the first invariant, I_1 (Yeoh 1993). In the same manner as the Ogden and polynomial models, this model is based on a series expansion (Selvadurai, 2006). The Yeoh model is also called the reduced polynomial model, and for compressible rubber is given by

$$W = \sum_{i=1}^3 C_i (I_1 - 3)^i \quad (6)$$

With a good fit over a large strain range, the Yeoh model can simulate various modes of deformation with only limited data, so leading to reduced requirements for material testing.

3. Materials and methods.

3.1 Material

The fibre-reinforced composite material used in this study was supplied by Trelleborg Dunlop GRG Holdings, Ltd. (Manchester, UK). The material was manufactured to 5 mm nominal thickness, and was supplied as a flexible composite sheet comprising a carbon-black filled vulcanised PVC/nitrile elastomeric matrix reinforced with nylon continuous weave cord fabric of orthogonal warp and weft architecture (see Figure1).

Scaled images of transverse sections of the composite material were obtained using an optical microscope fitted with an AxioCam digital acquisition system (Zeiss Stemi, Zeiss GmbH). The composite volume fractions were measured to be 0.89 PVC/nitrile phase and 0.11 nylon fibre phase.

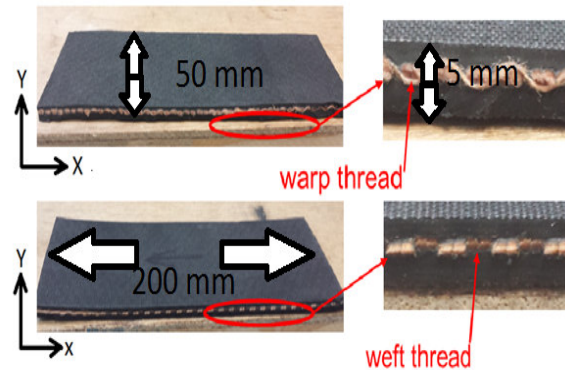


Figure (1) Specimen geometry and cross sections of the composite material showing the warp and weft arrangements of the nylon reinforcement fibres

3.2 Experimental procedure

3.2.1 Video gauge derived strain measurement

Using uniaxial tension and planar shear test methods, sample deformational behaviour was investigated using a non-contact optical method based upon a video extensometer gauge, VG (Imetrum, Bristol, UK). The VG system was used to capture multiple strain measures (multiple regions of interest) from the sample surface during testing. The results reported in this study were limited to two-dimensional (in-plane) measures of surface displacement, and were acquired using a single camera focussed on the sample surface during testing (see Figure 2). The strain data-sets arising from the video images were processed using a commercial software package (Imetrum, Bristol, UK).

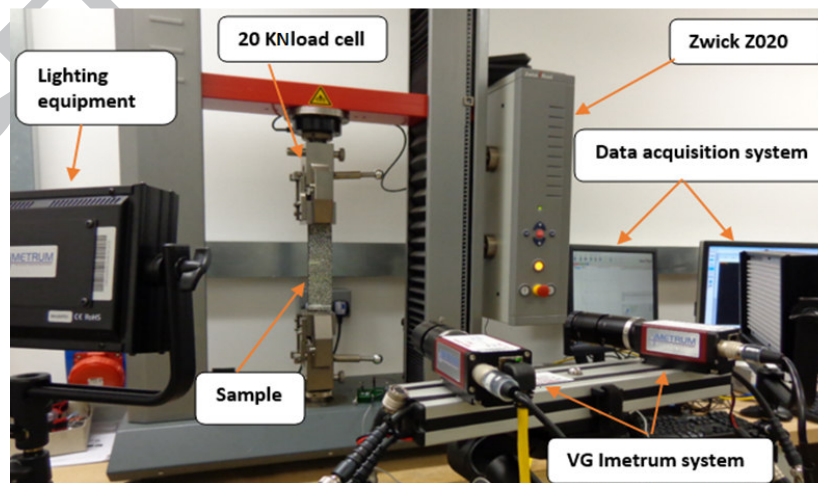


Figure (2) Experimental set-up showing VG system and sample position within the tensile testing frame.

The underpinning technology for the VG image analysis system used is that of that of Digital Image Correlation (DIC), which is a widely utilised optical measurement technology (Pan et al., 2009).

3.2.2 Uniaxial tensile loading of composite fabric

A uniaxial tension test was performed on samples of size $200 \times 50 \times 5$ mm. Tests were carried out at room temperature and were performed on ten specimens of the composite: five were loaded in parallel to the weft fibre direction and five were loaded in parallel to the warp fibre direction. Uniaxial tension was applied using a Zwick Z020 (Zwick GmbH) universal testing machine, to applied maximum loads of 6 kN. Each specimen of the composite was uniaxially stretched at a cross-head extension rate of 100 mm/min. Load and extension data were recorded at a frequency of 10 data per second, from which nominal stress and strain data were calculated based on sample original cross-sectional area and gauge length.

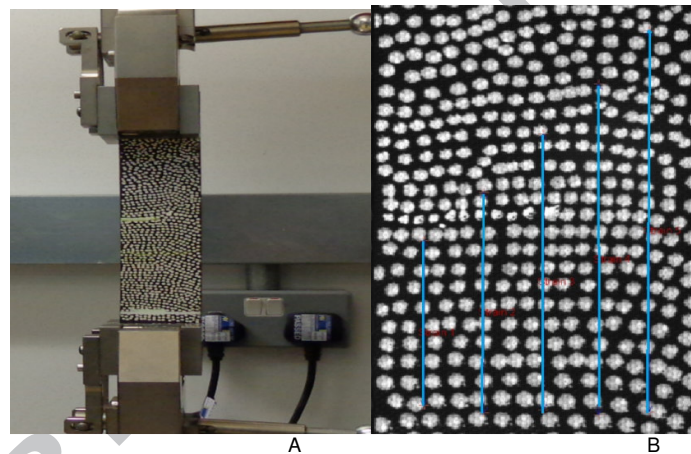


Figure (3). A, Test mode for specimens loaded parallel to the fibre (warp or weft) direction. B, strain gauges longitudinally aligned with the uniaxial tension load direction (Sample has been prepared with a speckle surface pattern).

To enhance contrast, samples were prepared with a speckle pattern and on each, five VG optical gauge lengths were defined longitudinally within the tested gauge length, from which measures of true strain during testing were obtained (Figure (3B)).

3.2.3 Pure shear loading of composite fabric

Pure shear (wide strip) geometry was employed (BS 903-5:2004) on composite samples of dimension $200 \times 40 \times 5$ mm loaded in tension in a Zwick Z020 universal testing machine. Six samples of the composite were tested: three were loaded in parallel to the weft fibre direction and three were loaded in parallel to the warp fibre direction. A 100 mm/min cross-head extension rate was used during the testing. The VG system was used to measure strain at six positions on the surface of each sample during loading (Figure (4)). For both warp and weft specimen orientations, shear strain measurements were taken from the in-

plane distortions of strain gauge elements orientated at +45 and -45 degrees to the axis of uniaxial tension. In the wide strip sample, uniaxial tension acting in the Y direction with respect to the rotated VG element (Figure 4) generates an equivalent stress state to that of equal and opposite principal normal stresses acting on the element. Measured nominal stresses applied during testing can therefore be converted to their equivalent shear stresses by application of a factor of 0.5. The shear strain (γ) measurements were generated from VG locations within the constrained central region of the sample, from an area of dimensions 100 x 40 mm.

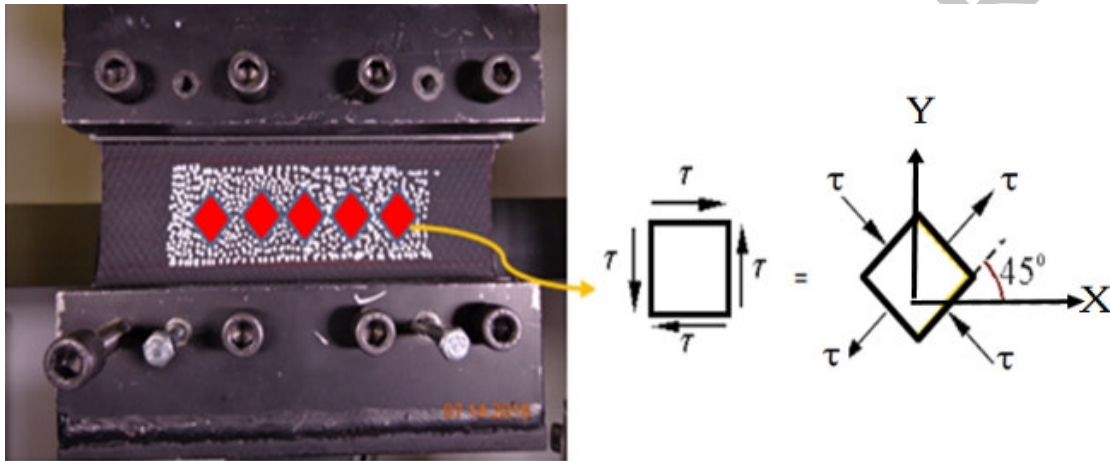


Figure (4) Wide strip (pure shear) specimen geometry showing the six VG locations and the equivalent stress state

Additional to direct measurement of shear strain, Figure (4) X and Y orientated VG strain gauges were used to obtain a measure of strain using the conventional plane strain transformation (45° strain gauge rosette) expression, namely

$$\gamma_{xy} = 2 \varepsilon_{45} - \varepsilon_x - \varepsilon_y \quad (7)$$

Where ε_{45} is the normal strain at 45° to the x- axis, ε_x is the normal strain in the x- axis and ε_y is the normal strain in the Y- axis, as defined in Figure (5).

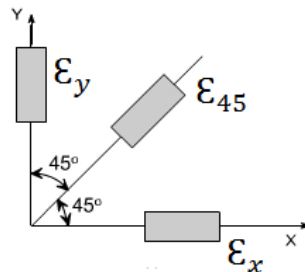


Figure (5): strain gauge rosette individual gauge orientations

Furthermore, in tensile loading, the elastic moduli (E) and Poisson's ratio (ν) of the warp and weft fibre directions can be related to each other (Barbero, 2010; Kraft et al., 2014) according to

$$\frac{\nu_{warp}}{E_{warp}} = \frac{\nu_{weft}}{E_{weft}} \quad (8)$$

This study explores the composite fabric elastic behaviour using data generated from two methods, from five samples loaded parallel to the weft direction and from five samples loaded parallel to the warp direction. The first method uses a manually defined optical strain gauge (longitudinal and transverse aligned uniaxial gauges) and the second method uses a software generated (image processing) measurement of ν . Because the behaviour of materials that exhibit a nonlinear elastic stress-strain response can depend upon on the acting stress/strain regime (ASTM E111-04, 2004; Mamlouk and Zaniewski, 2010), the chord elastic modulus was used to distinguish between different regimes (responses) of the fabric material.

4. Experimental Results and Discussion

Figure (6) shows the results of uniaxial testing stress-strain behaviour measured by VG for samples loaded in parallel to each of the weft and warp fibre directions. At 6 kN load (23 MPa nominal stress) the strains (stretches) in the weft direction were lower than those in the warp direction. The average values obtained were 12% and 26 % for stretch in the weft and warp directions respectively. Both sample orientations demonstrate non-linear (hyperelastic) behaviour.

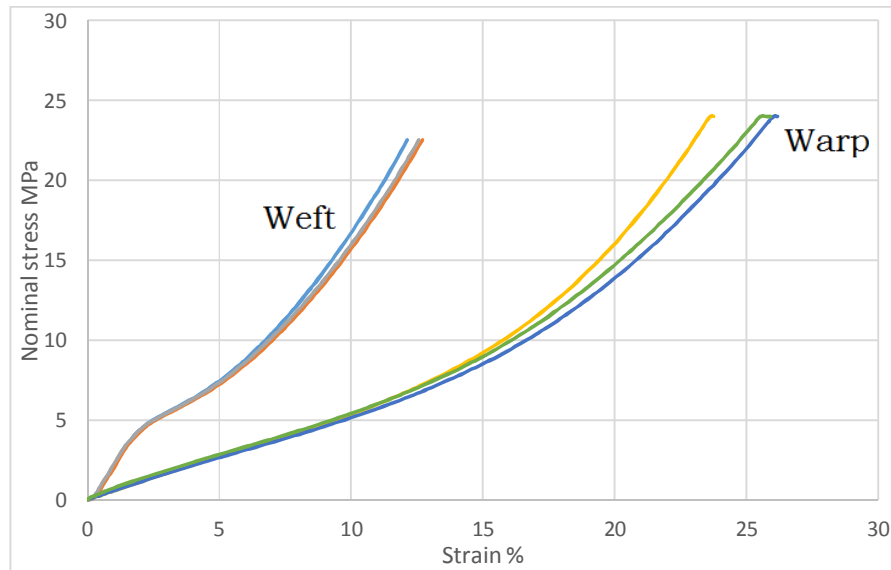


Figure (6): Uniaxial testing stress–strain graph for composite specimens loaded parallel to the weft and warp fibre directions

Figure (6) shows that the uniaxial tensile testing of the composite specimens loaded parallel to the weft direction elongated less than specimens loaded parallel to the fibre warp direction. The material shows a stiffer response in the weft direction, with strain in the warp direction more than double that of the weft direction for much of the test.

Figure (7) shows the sample results of the wide strip test derived true shear strain. The stress-strain curve deviated from linear beyond an applied nominal stress of 2.5 MPa (1.25 MPa of applied shear stress), for the samples loaded parallel to the weft fibre direction. However, for the samples loaded in parallel to the warp fibre direction, this linear to non-linear transition in material behaviour was less marked, and occurred at a lower nominal stress of 1 MPa (equivalent to 0.5 MPa of applied shear stress).

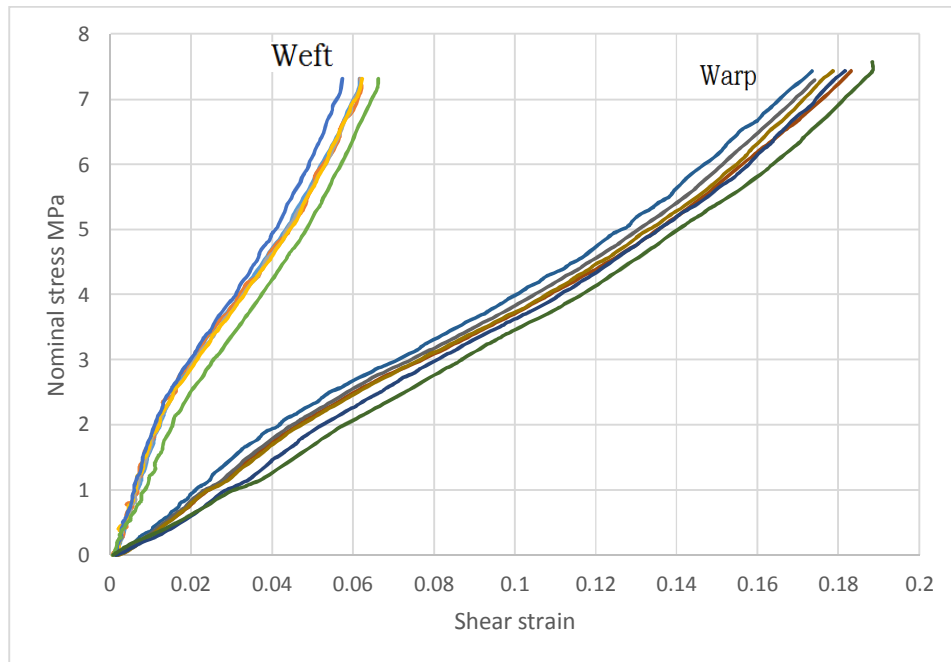
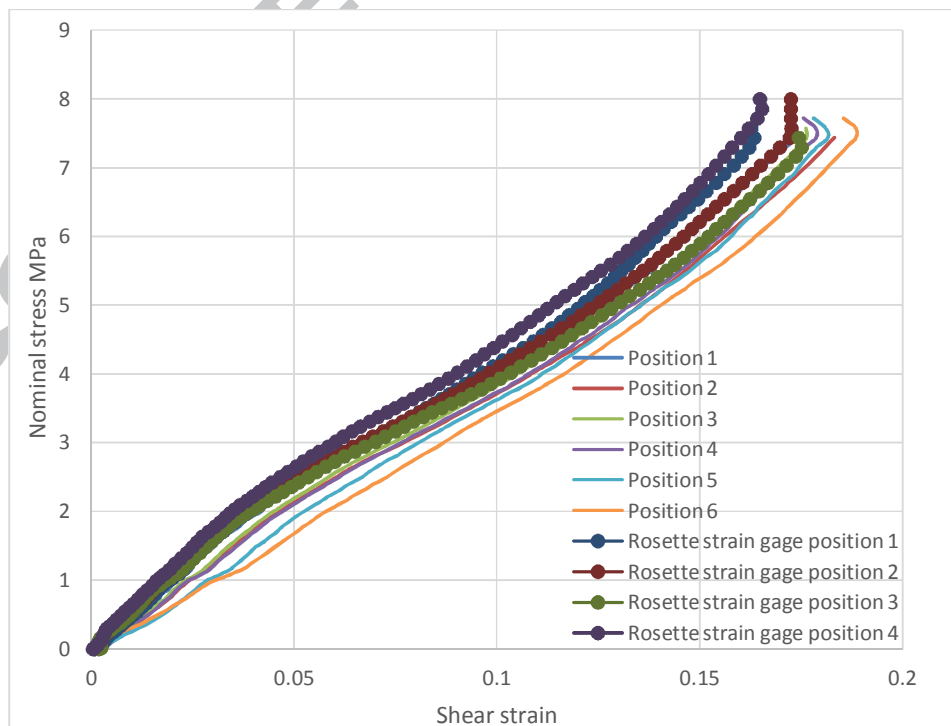


Figure (7): planar shear oriented stress vs strain behaviour for fibre-filled composite specimens loaded parallel to the weft and warp fibre directions

Using equation (7) the strain rosette derived shear strains shown in Figure (8) were calculated. This figure also shows the directly measured shear strain obtained from six central locations within the planar shear region for the fabric loaded parallel to the warp direction. Figure (8) compares the results obtained from the VG for shear strain and the calculations for the rectangular rosette, using equation (7) above.



Figures (8): Shear strain response derived from direct results and rosette strain gauges for the warp direction of fabric loading

These results show that the shear strain measured on both orientations of fabric can be seen to increase non-linearly with respect to extent of applied load. This behaviour can be attributed to the effect of reinforcement fibre crimping. The crimp value reduces in the loading direction and increases in the transverse direction and continues until the yarns in the loading direction become straight or the yarns in the transverse direction reached a jammed state (Testa and Yu, 1987; Potluri and Thammandra, 2007).

With regards to Poisson's ratio ν , Figure (9) shows the averaged ν behaviour from the sample loaded along the weft and warp fibre directions. The highest ν was around 0.36 for the samples loaded parallel to the warp direction and around 0.18 for the samples loaded parallel to the weft direction.

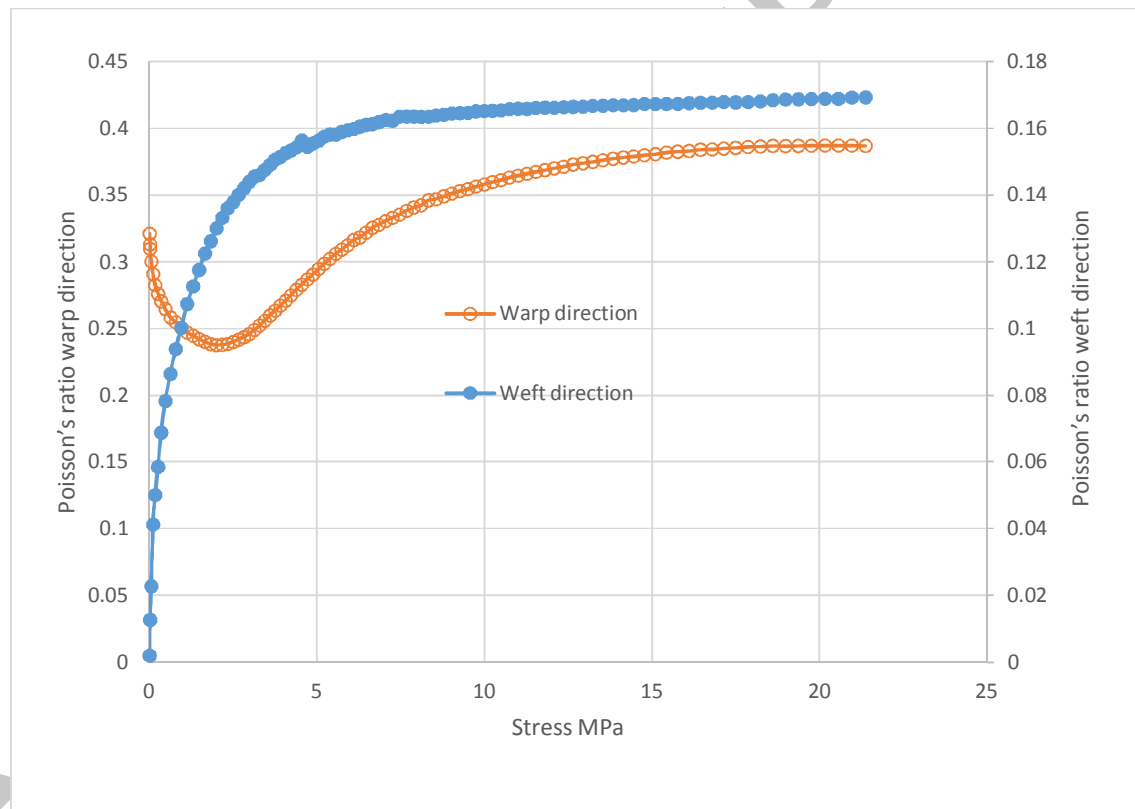


Figure (9): Average Poisson's Ratio, ν for composite specimens loaded parallel to the weft (RH axis) and warp (LH axis) fibre directions.

The stress-strain relations observed show two distinctive regimes, i.e., primary and secondary zones, and these were defined from analysis of the stress strain graphs obtained

from the tested material. The primary and secondary chord moduli for specimens loaded parallel to the weft and warp fibre directions were calculated using (Siddiqui et al., 2012):

$$E = \frac{P_u - P_l}{A(\varepsilon_u - \varepsilon_l)} \quad (9)$$

where, E is the primary and secondary chord modulus, as defined in Figures (10) and (11); A is the cross-sectional area; P_u is the tensile load at the upper strain limit; P_l is the tensile load at the lower strain limit; ε_u is the upper strain limit; and ε_l is the lower strain limit. Table 1 summarises the primary and secondary chord modulus results obtained.

Elastic Properties	Weft direction of loading	Warp direction of loading
Poisson's ratio ν (manually derived from optical strain gauges)	0.17	0.37
Poisson's ratio ν (software derived)	0.18	0.36
Primary chord modulus	0.59 MPa	1.6 MPa
Secondary chord modulus	1.6 MPa	2 MPa

Table 1 Summary of Poisson's ratio and modulus measures of the composite fabric

Table 1 shows that the composite exhibits a higher modulus when loaded parallel to the weft fibre direction than when loaded parallel to the warp fibre direction and also that the measured ν ratio differ with respect to fibre orientation. In both cases, ν for samples loaded parallel to warp direction were found higher than those loaded parallel to the weft direction. By comparison, use of equation (8) produced $\nu_{weft} = 0.11$ and $\nu_{warp} = 0.62$ for the two different directions of loading with respect to the reinforcement fibre orientation. Use of equation (8) provides a useful check on the validity of the experimental data and although the two methods produced different values for ν_{weft} and for ν_{warp} , they were considered to be within the margin of experimental error. Furthermore, literature values for ν lying in the range of 0.2 to 0.5 for similar materials to those contained within the composite bracket the measured values obtained in this study (Hursa et al., 2009; Kraft, et al., 2014).

The experimental results from the uniaxial extension and wide strip tension (pure shear) tests were used to identify a constitutive material model, for material model parameter estimation, and for material model verification.

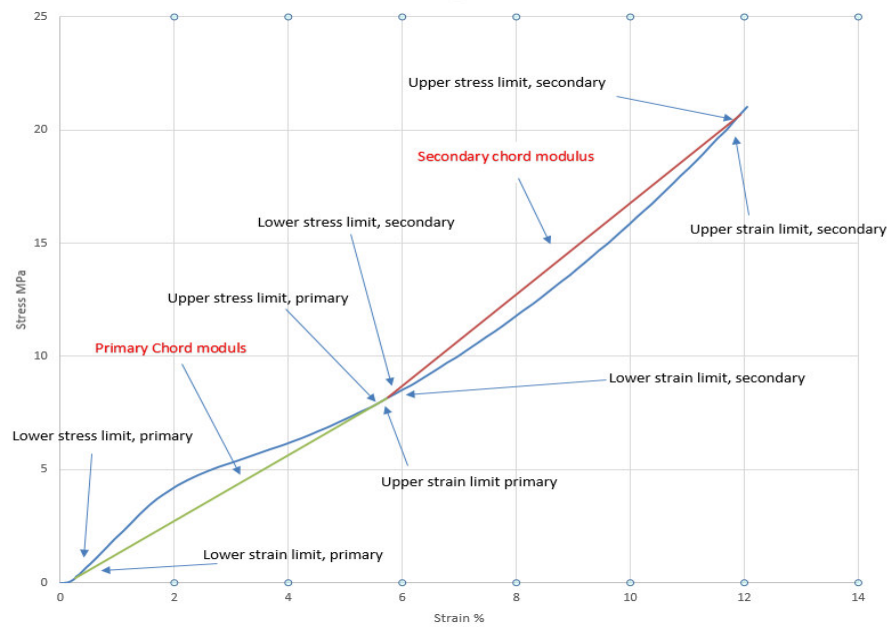


Figure 10: Uniaxial tensile stress-strain graph for composite specimens loaded parallel to the weft fibre direction

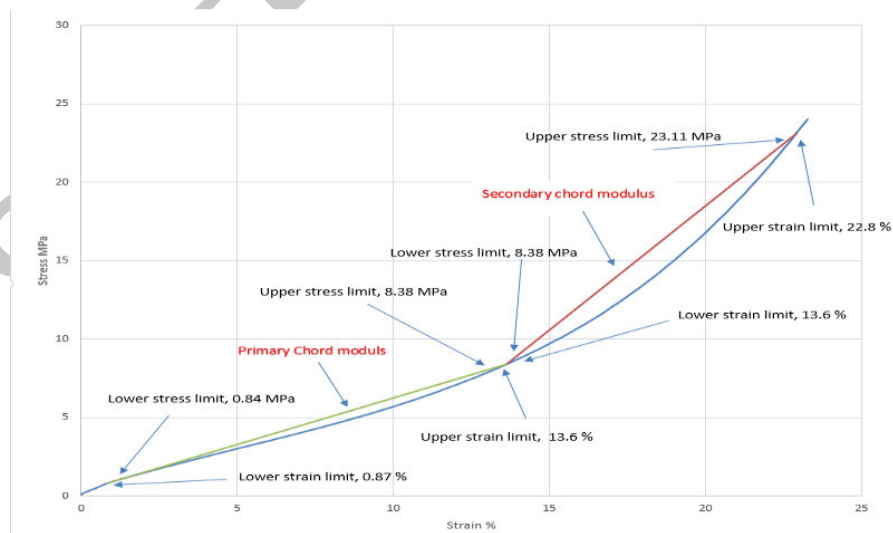


Figure 11: Uniaxial tensile stress-strain graph for composite specimens loaded parallel to the warp fibre direction

5. Curve Fitting and Experimental Results.

ABAQUS commercial software has hyperelastic materials modelling capability. Experimental data are introduced and the relevant coefficients of selected hyperelastic materials models that best fit the experimental data identified (Ruiz and Gonzalez, 2006). A nonlinear least squares regression is performed to determine the hyperelastic constants, and this is then iterated to obtain a best fit to the data-set (Motulsky and Ransnas 1987). The least-squares error is minimized, using absolute and relative errors, respectively, given by

$$\text{Absolute error} = \sum_i [\text{experimental data } (i) - \text{calculated data } (i)]^2 \quad (10)$$

$$\text{Relative error} = \sum_i \left[1 - \frac{\text{experimental data } (i)}{\text{Calculated data } (i)} \right]^2 \quad (11)$$

Using experimental data obtained from the uniaxial tension and wide strip tension (pure shear) tests, ABAQUS (ABAQUS, 1992) was used to model the material behaviour, based upon the assumption of a hyperelastic material model behaviour, and the fact that the composite contains a high volume fraction of isotropic hyperelastic matrix material. Fits of the data to the Ogden and the Yeoh materials models were investigated in this work. The results of this modelling are given in Figures (12) and (13) show the Ogden (order N1, N2 and N3 material model parameters) and Yeoh with (order N3 material model parameters), which produced the best fits the experimental data for samples loaded in parallel to the weft direction. In Figures (14) and (15) for samples loaded in parallel to the warp direction, the Ogden (with order N1 material model parameters) and Yeoh with (with order N2 and N3 material model parameters) best fit the experimental data. The results from the ABAQUS model fitting are summarised in Tables 3 and 4.

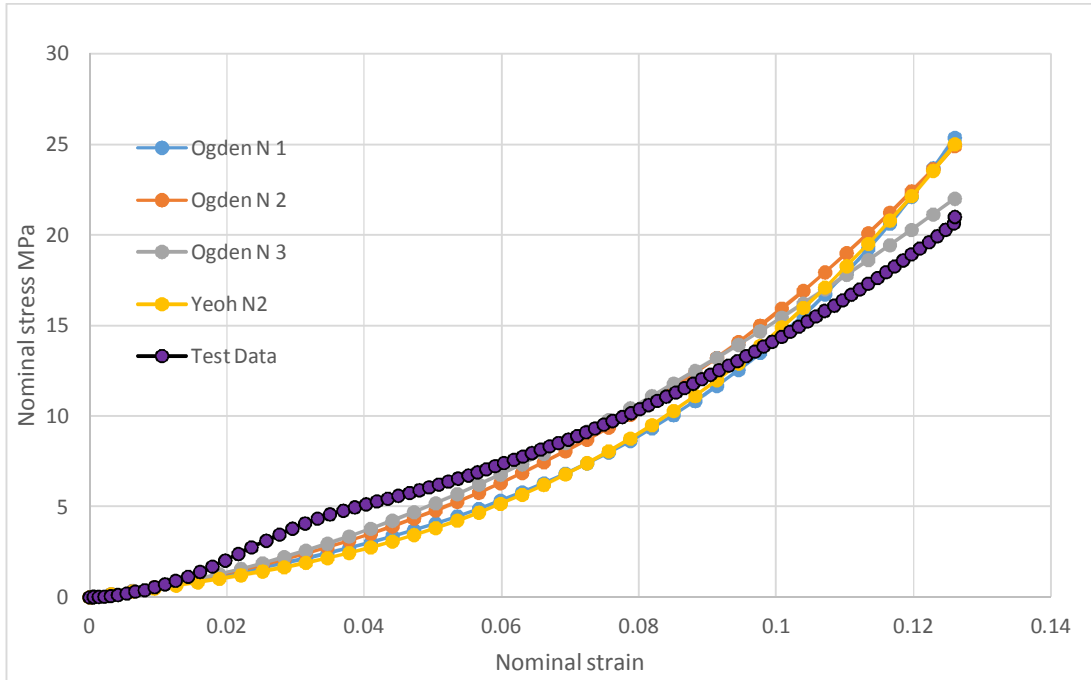


Figure (12): Fitting of different hyperelastic models with uniaxial data from samples loaded parallel to the west direction

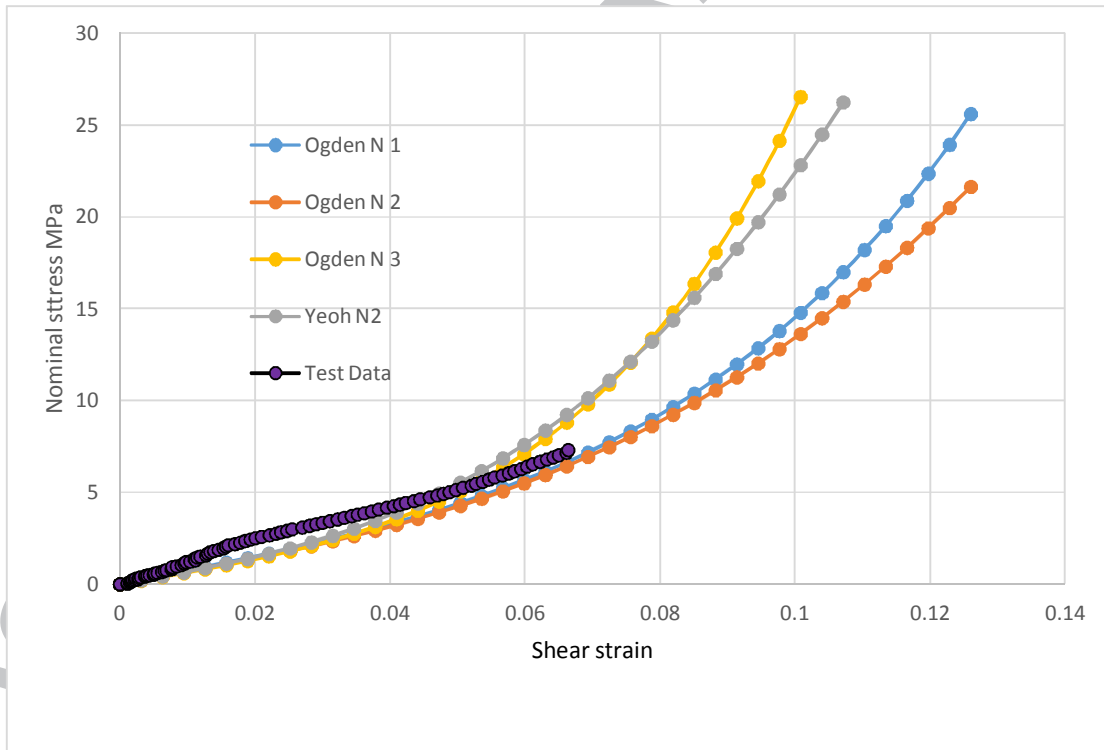


Figure (13): Fitting of different hyperelastic models with planar data from samples loaded parallel to the west direction

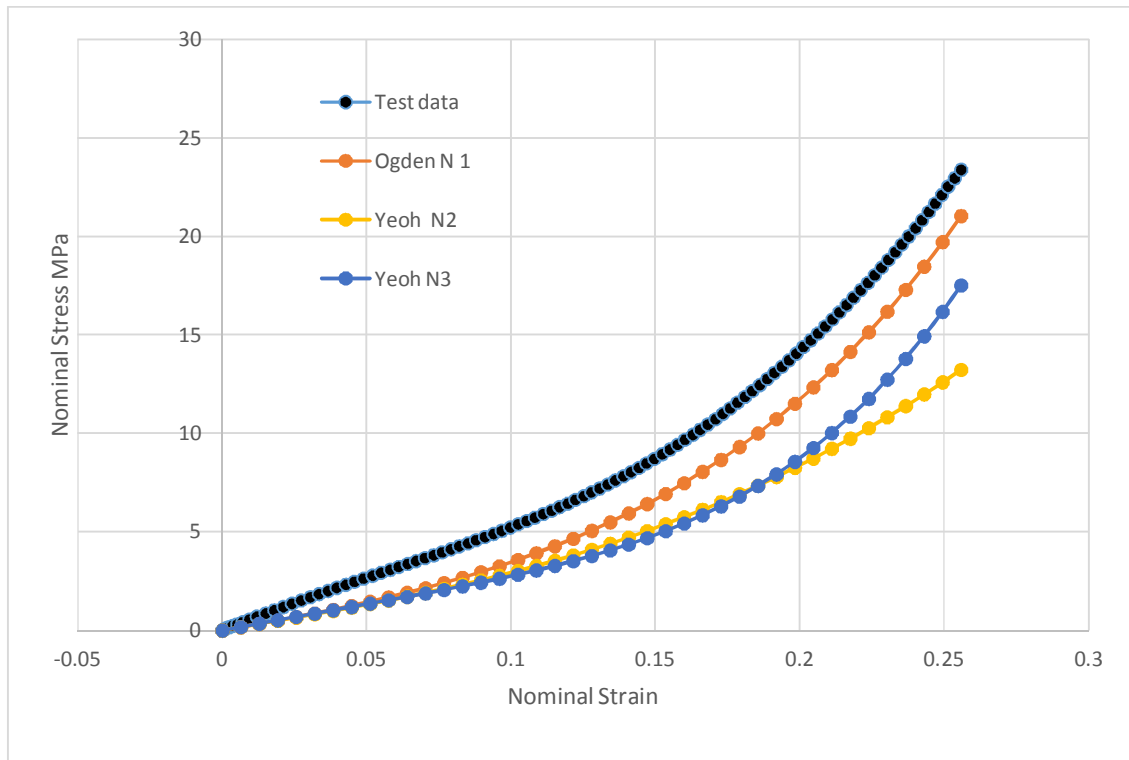


Figure (14): Fitting of different hyperelastic models with uniaxial data from samples loaded parallel to the warp direction

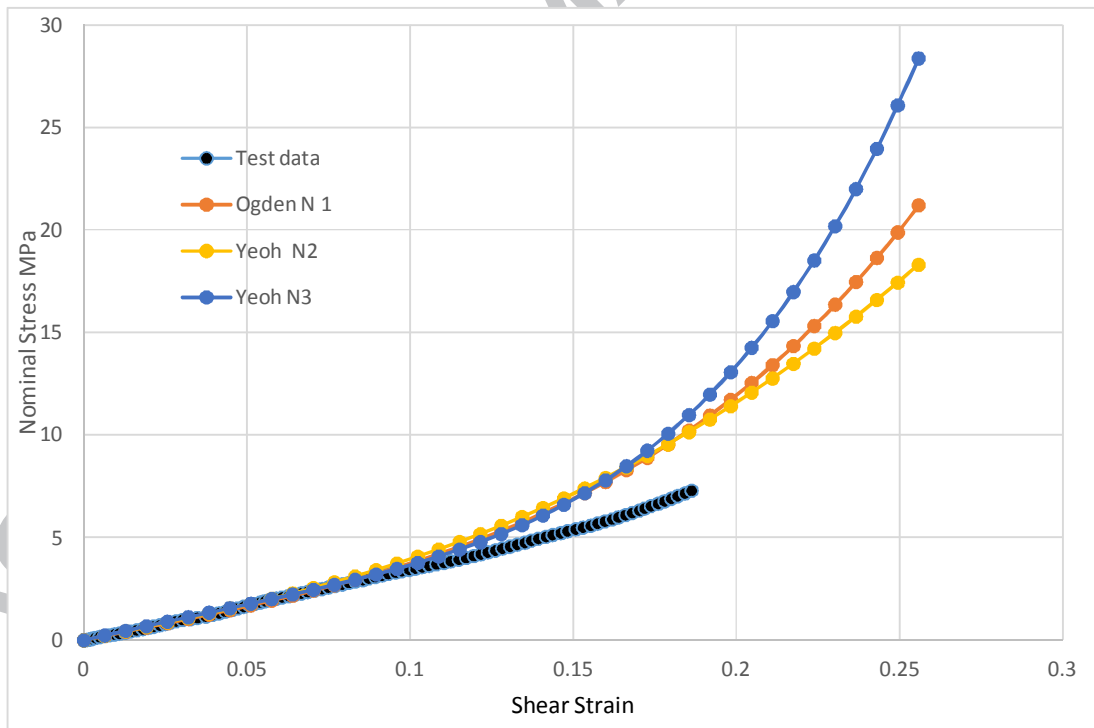


Figure (15): Fitting of different hyperelastic models with planar data from samples loaded parallel to the warp direction

Hyperelastic model	constants	Least squared error
Ogden N 1	$\mu_1 = 18.60 \quad \alpha_1 = 25.00$	40.21 %
Ogden N 2	$\mu_1 = 417.55 \quad \alpha_1 = -400.21$	38.67 %

	$\mu_2 = 8.26 \quad \alpha_2 = 6.13$	
Ogden N 3	$\mu_1 = -2672.08 \quad \alpha_1 = -10.35$ $\mu_2 = 1695.67 \quad \alpha_2 = -6.39$ $\mu_3 = 992.35 \quad \alpha_3 = -15.58$	36.74 %
Yeoh N 2	$C_{10} = 8.48 \quad C_{20} = 324.44$	

Table 4: Results of fitting using uniaxial tension and pure shear data for samples loaded parallel to the weft fibre direction

Hyperelastic model	constants	Least squared error
Ogden N 1	$\mu_1 = 8.31 \quad \alpha_1 = 13.50$	31.15 %
Yeoh N 2	$C_{10} = 4.31 \quad C_{20} = 18.66$	
Yeoh N 3	$C_{10} = 4.59 \quad C_{20} = 3.93 \quad C_{30} = 94.54$	

Table 5: Results of fitting using uniaxial tension and pure shear data for samples loaded parallel to the warp fibre direction

6. Conclusions

This work describes a novel investigation of the mechanical properties of a fibre-reinforced composite consisting of carbon-black filled vulcanised PVC/nitrile compound and nylon cord fabric of two-directional warp and weft, by means of optical methods applied to uniaxial and wide-strip tension tests. These tests were carried out at room temperature to assess the suitability of the material for structural applications. Non-contacting optical methods (using a video strain gauge) were found to be convenient for measurement of large deformations, for example where the application of other strain measurement techniques would become difficult or unfeasible. With a non-contacting optical system, it is possible to take measurements at multiple points within the loaded gauge section, and gather data in real-time. In this respect, the tested composite investigated in this work showed anisotropic material behaviour whereby loading in the weft direction invoked higher stiffness than loading in the warp direction. This result is to be expected, and is typical of fibre-filled elastomeric materials, whereby the fibre architecture dominates the load deformation response. The non-contact VG technique used was found useful to quantify this behaviour for strains (stretches) of up to 0.25 in uniaxial loading and up to 0.18 in wide-strip planar tension. This was used in this study to determine normal strain, shear strain and Poisson's ratio. Overall, the measured strain and shear strain for specimens loaded parallel to the warp fibre direction were generally higher than for specimens oriented in the weft direction. The composite demonstrated anisotropic material behaviour, confirmed by the various test results obtained for the composite loaded parallel to the weft and warp fibre directions, and also non-linear stress-strain response was observed for all the test conditions considered. Furthermore, experimental data from the tests were obtained and used as input to ABAQUS

software in order to calibrate hyperelastic constitutive models of the PVC/nitrile behaviour. Among the various hyperelastic material models included within commercial FE codes, the Ogden and Yeoh relationship were found to best model the experimental data over the extension regimes studied, giving the closest agreement between numerical fit and experimental data.

ACCEPTED MANUSCRIPT

References

- ABAQUS: Theory Manual 6.12, (1992) Hibbitt, Karlsson & Sorensen Inc., Providence, RI, USA.
- Aboshio, A., Green, S., & Ye, J. Q. (2014). New constitutive model for anisotropic hyperelastic biased woven fibre reinforced composite. *Plastics, Rubber and Composites*, 43(7), 225-234.
- Ali, A., Hosseini, M., & Sahari, B. B. (2010). A review of constitutive models for rubber-like materials. *American Journal of Engineering and Applied Sciences*, 3(1), 232-239.
- ASTM E111-04, (2004) Standard Test Method for Young's Modulus, Tangent Modulus, and Chord Modulus, ASTM International, West Conshohocken, PA.
- Barbero, E. J. (2010). *Introduction to composite materials design*. CRC press, Boca Raton.
- Boyce, M. C., & Arruda, E. M. (2000). Constitutive models of rubber elasticity: a review. *Rubber chemistry and technology*, 73(3), 504-523.
- BS 903-5:2004 Physical testing of rubber. Guide to the application of rubber testing to finite element analysis. (2004) BSI, London.
- Gent, A.N., (1992). *Engineering with Rubber*, Hanser Publishers, New York.
- Hardiman, C.J., McKenzie, G.T. and Stiberth, L.T. (2000). Nitrile rubber/polyvinyl chloride blends. U.S. Patent No. 6,043,318.
- Hursa, A., Rolich, T., & Ražić, S. E. (2009). Determining pseudo Poisson's ratio of woven fabric with a digital image correlation method. *Textile Research Journal*, 79(17), 1588-1598.
- Holzappel, G.A., Gasser, T.C., and Ogden, R.W. (2000) *Journal of Elasticity*, 61, 1-48.
- Jacobsen, A. J., Luo, J. J., & Daniel, I. M. (2004). Characterization of constitutive behaviour of satin-weave fabric composite. *Journal of Composite Materials*, 38(7), 555-565.
- Jones, D.F. and Treloar, L.R.G., 1975. The properties of rubber in pure homogeneous strain. *Journal of Physics D: Applied Physics*, 8(11), 1285–1304.

Kraft, S. M., Moslehy, F. A., Bai, Y., & Gordon, A. P. (2014). Characterization of the orthotropic elastic constants of a micron woven wire mesh via digital image correlation. *Experimental Mechanics*, 54(4), 501-514.

Mamlouk, M.S. and Zaniewski, J.P. (2010). *Materials for Civil and Construction Engineers*, 4th Edition, Pearson, London.

Motulsky, H. J., & Ransnas, L. A. (1987). Fitting curves to data using nonlinear regression: a practical and nonmathematical review. *The FASEB journal*, 1(5), 365-374.

Ogden, R.W. (1972). Large deformation isotropic elasticity—on the correlation of theory and experiment for the compressible rubberlike solids. *Proceedings of the Royal Society of London A*. 1972; 328(1575), 565-584.

Pan, B., Qian, K., Xie, H., & Asundi, A. (2009). Two-dimensional digital image correlation for in-plane displacement and strain measurement: a review. *Measurement Science and Technology*, 20(6), 6-20.

Potluri, P., and Thammandra, V. S. (2007). Influence of uniaxial and biaxial tension on meso-scale geometry and strain fields in a woven composite. *Composite Structures*, 77(3), 405-418.

Reese, S., Raible, T., Wriggers, P. (2001). Finite element modelling of orthotropic material behaviour in pneumatic barriers. *Int. J. Solids and Struct.* 38 (52) p9525-9544

Ruiz, M.J.G. and Gonzalez, L.Y.S. (2006) Comparison of hyperelastic material models in the analysis of fabrics. *International Journal of Clothing Science & Technology*. 18. 314-325.

Seibert, D.J. and Schoche, N. (2000). Direct comparison of some recent rubber elasticity models. *Rubber Chem. Technol.*, 73: 366-384.

Selvadurai, A. (2006). Deflections of a rubber membrane. *Journal of the Mechanics and Physics of Solids* 54(6), 1093–1119.

Shahzad, M., Kamran, A., Siddiqui, M. Z., & Farhan, M. (2015). Mechanical characterization and FE modelling of a hyperelastic material. *Materials Research*, 18(5), 918-924.

Siddiqui, M.Z., Tariq., Naz, N and Ahmed, M.F. (2012) *J Space Tech.* 1. 32-37.

Testa, R., and Yu, L. (1987). Stress-strain relation for coated fabrics. *Journal of Engineering Mechanics*; 113(11):1631.

Treloar, L.R.G. (1973). The elasticity and related properties of rubbers. Reports on progress in physics, 36, 755-826.

Treloar, L.R.G (1958). The physics of rubber elasticity. 2nd ed. Oxford University Press.

Yang, H., Yao, X. F., Ke, Y. C., Ma, Y. J., & Liu, Y. H. (2016). Constitutive behaviours and mechanical characterizations of fabric reinforced rubber composites. Composite Structures, 152, 117-123

Yeoh, O. H. (1993). Some forms of the strain energy function for rubber. Rubber Chemistry and Technology, 66(5), 754-771.

ACCEPTED MANUSCRIPT